Membrane Stress and Permeabilization Induced by Asymmetric Incorporation of Compounds

Heiko Heerklotz
Department of Biophysical Chemistry, Biocenter of the University of Basel, CH-4056 Basel, Switzerland

ABSTRACT The area balance or imbalance between the inner and outer monolayer of biological membranes is a key parameter for driving shape changes (including exo and endocytosis) and controlling the bilayer curvature stress. The asymmetric incorporation of a drug or biological agent interferes with these processes, and the subsequent stress may lead to a membrane permeation or permeabilization. A main goal of this study is to introduce new methods to characterize such phenomena using isothermal titration calorimetry. POPC unilamellar vesicles and a series of alkyl maltosides are used as model systems; the unilamellarity was checked by NMR with the shift reagent Pr^{3+}. The free energy, enthalpy, and entropy associated with the asymmetry stress are estimated by comparing partitioning data of uptake versus release assays. The asymmetry stress is of enthalpic nature and somewhat reduced by entropic effects. Stimulated membrane permeation occurs at a mean maltoside-to-lipid ratio of ~0.2, which corresponds to an apparent area asymmetry of ~30% and a limiting free energy of the order of 2 kJ/mol of maltoside. Membrane solubilization to coexisting micelles proceeds at mole ratios of ~0.73, 0.81, and 0.88 (C_{12}-, C_{13}-, and C_{14}-maltoside, respectively). Experiments with vesicles pre-loaded with surfactant in both monolayers provide evidence that the translocation threshold is controlled by the asymmetrically incorporated surfactant, whereas the onset of solubilization depends on the total surfactant content in the membrane. Free copies of the uptake and release fitting script including instructions are available upon request to heerklotz@gmx.net.

INTRODUCTION

Bilayer couple concept

The uptake of drugs or other solutes into biological or model membranes may increase the area requirement of the outer monolayer, whereas the inner monolayer tends to maintain its area requirement if the solute does not translocate into it. Sheetz and Singer (1974) have compared the fact that asymmetric area expansion tends to curve a bilayer with a bimetallic couple (bilayer couple hypothesis). However, changes in the local curvature of plasma membranes or lipid vesicles are constrained by the fact that these areas are closed and changes of the enclosed volume (by water exchange with the outside) are opposed by osmotic effects. Thus, consequences of asymmetric uptake of solutes into membranes are 1) the creation of mechanic stress, which 2) reduces the affinity for further incorporation, and 3) drives shape changes. At a certain limit, the energy stored in the stress promotes the 4) translocation of molecules to the inner monolayer.

New techniques

The aim of the current study is to introduce new experimental approaches based on isothermal titration calorimetry that serve to answer the following questions. What is the driving force for asymmetry-driven membrane translocation of originally impermeable substances to the inner monolayer? How large is the energy of the bending stress and which are the enthalpic versus entropic contributions to it? Does the partition coefficient for asymmetric uptake differ substantially from that for balanced incorporation? How can the translocation threshold of a solute be measured without specific labeling, and at which apparent area asymmetry does it occur? Does the translocation of the solute permeabilize the membrane to other aqueous solutes as well? The issues of membrane deformation, permeation, and permeabilization are of major relevance for the understanding of physiological effects and applications as outlined in the following.

Deformations

The area balance or imbalance between the two monolayers is one of the key properties of biological membranes. There is good evidence that it is actively regulated by transmembrane pumping or directed synthesis of, e.g., lipids to govern deformations initiating both endo and exocytosis and other physiologically required shape changes of cells (Rauch and Farge, 2000; Farge et al., 1999; Mui et al., 1995; Farge, 1994; Sackmann et al., 1986). Asymmetric incorporation of solutes interferes with these processes. Treatment of erythrocytes with impermeable amphiphiles such as dodecyl maltoside drives echinocytosis and exovesiculation, whereas preferential expansion of the inner monolayer causes stomatocytosis and endovesiculation (Bobrowska-Hagerstrand et al., 1999; Schwarz et al., 1999; Hagerstrand and Isomaa, 1992). Most reports on the elastic properties and deformations of membranes are based on the visualiza-

Received for publication 11 August 2000 and in final form 20 March 2001.
Address reprint requests to Dr. Heiko H. Heerklotz, Dept. of Biophysical Chemistry, Biocenter of the University of Basel, Klingelbergstrasse 70, CH-4056 Basel, Switzerland. Tel.: 41-61-2672192; Fax: 41-61-2672189; E-mail: heiko.heerklotz@unibas.ch.

0006-3495/01/07/184/12 $2.00

tion of cells or giant liposomes and the micropipette aspiration technique (Olbrich et al., 2000; Rawicz et al., 2000; Evans and Needham, 1987). The methods applied here yield no direct information about deformations but the measurement of the energy, enthalpy, and entropy of asymmetric incorporation provides clues on the balance between dilation and deformation of the membrane.

Permeation

There are different pathways for the permeation of drugs into cells. Hydrophobic molecules partition into the core of the membrane and can be released to the cytoplasm from there. Hydrophilic compounds are typically taken up via endocytosis (cf. above). Others are transported via specific carrier proteins. Molecular "cargoes," which are covalently attached to certain, often lysine- or arginine-rich transporter peptides such as tat-derived peptides, penetratins, or transportan, are internalized into eukaryotic cells by means of a so-far unknown mechanism (Lindgren et al., 2000). This study aims to contribute to a more detailed understanding of asymmetry-driven flip-flop of originally impermeable molecules, which might be another pathway of unspecific membrane permeation of amphiphiles. It must be noted that the flip-flop of solutes across membranes is not easily measured. Kragh-Hansen et al. (1998) have used radiolabeled detergents for detecting whether or not certain detergents flip-flop out of multilamellar lipid vesicles. The choice of alkyl maltosides as model systems for our study is based on their result that dodecyl maltoside does not translocate across lipid bilayers within hours.

Permeabilization

The stress in the asymmetrically expanded bilayer may also lead to membrane permeabilization, i.e., a local destruction of the membrane leading to an exchange of all (not too large) aqueous solutes between the outside and inside of the cell or vesicle. This has been discussed for charged detergents such as cholates (Schubert et al., 1983, 1986). Growing resistance of bacteria against classic antibiotics has led to large research efforts toward the understanding of antibiotic peptides. These accumulate in the outer monolayer of, e.g., bacterial membranes, and kill the target cell upon translocation to the inner monolayer. The details of the latter phenomenon are an issue tackled by quite a number of, partially competing, models (for recent studies cf. Wieprecht et al., 1999; Vogt et al., 2000; Uematsu and Matsuzaki, 2000; Shai, 1999; Huang, 2000; Bechinger, 1999). The relevance of asymmetric membrane expansion for this translocation is still unclear and the methods presented here are potentially suitable to approach this problem.

Fusion

Area asymmetry effects have also been discussed to play a role upon fusion of viruses with target cells mediated by insertion of amphiphilic fusion peptides into the membrane by Longo et al. (1998). They raise the question whether the stability limit for symmetric vesicle inflation (~5 area-percent) applies also to mechanical failure of vesicles upon asymmetric expansion by peptides. The present study shows that such a comparison is not straightforward.

MATERIALS AND METHODS

Materials

The lipid, 1-palmitoyl-2-oleoyl-*sn*-glycero-3-phosphocholine (POPC) was purchased from Avanti Polar Lipids, Alabaster, AL. The surfactants *n*-dodecyl-β-D-maltopyranoside (C_{12}-maltoside), *n*-tridecyl-β-D-maltopyranoside (C_{13}-maltoside) and *n*-tetradecyl-β-D-maltopyranoside (C_{14}-maltoside) were bought from Anatrace Inc., Maumee, OH in Anagrade purity (>99% HPLC). Prasoedymium nitrate was from Riedel del Haen. All substances were used without further purification.

Vesicle preparation

The lipid was dried from the storage solution, weighed, and dispersed in buffer (TRIS 10 mM + NaCl 100 mM, pH 7.4) by vortexing. After five freeze-thaw cycles, large unilamellar vesicles were prepared by 19 passages (back and forth) through two stacked Nuclepore polycarbonate membranes of 100 nm pore size in a 1 ml mini-extruder (MacDonald et al., 1991). The lipid concentration was confirmed by spot checks using a phosphate assay. The effective unilamellarity was checked by NMR (cf. below).

Isothermal titration calorimetry

The measurements were performed using a VP isothermal titration calorimeter produced by MicroCal Inc., Northampton, MA (Chellani, 1999). All fit procedures were performed with MicroCal Origin.

Partitioning experiment (uptake)

This protocol serves to measure the partition coefficient, K, and the molar enthalpy of transfer of detergent (D) from the free (f for free or w for "in water") to the membrane-bound (b) state, $\Delta H_D^{w\to b}$. The mole ratio partition coefficient relating the detergent-per-lipid mole ratio in the membrane, R_b, to the free detergent concentration, $C_{D,f}$

$$K \equiv \frac{R_b}{C_{D,f}} = \frac{C_{D,b}}{C_L^0 \cdot C_{D,f}} \tag{1}$$

is superior for detergent-lipid systems because it takes non-ideal mixing into account so that it is hardly dependent on the detergent content in the membrane (cf. Lasch, 1995; Heerklotz and Seelig, 2000b for a discussion of different definitions of K). The total detergent concentration is denoted C_D^0 and the concentration of bound detergent in the total volume is $C_{D,b}$. Rearrangement of Eq. 1 after substitution of $C_{D,f} = C_D^0 - C_{D,b}$ leads to the bound fraction of the detergent, ϕ (cf. Lasch et al., 1983):

$$\phi \equiv \frac{C_{D,b}}{C_D^0} = \frac{K\gamma C_L^0}{1 + K\gamma C_L^0} \tag{2}$$

The factor γ serves to correct the lipid concentration to the fraction that is actually accessible to the detergent. It amounts to 1 if the detergent can permeate the lipid bilayer and bind to both outer and inner monolayers. If the detergent cannot translocate to the inner monolayer, only the lipid in the outer monolayer "binds" detergent so that $\gamma = 0.5$ for large unilamellar vesicles.

For the ITC uptake experiment, the cell is filled with 1.4 ml of a detergent solution of concentration C_D^0 well below the critical micelle concentration (cf. Table 1). The concentration of bound detergent, $C_{D,b} = \phi \cdot C_D^0$, is zero because $\phi = 0$ in the absence of lipid. The syringe is filled with a lipid vesicle dispersion of concentration C_L^{syr} (typically 15 mM) and a series of injections of some microliters each are performed into the cell. C_D^0 remains constant except for a small correction accounting for replacement of some cell content by the injected volume. The variation of ϕ upon lipid titration (from 0 to 1) is given by the first derivative of Eq. 2:

$$\phi' \equiv \frac{1}{C_D^0} \cdot \frac{\partial C_{D,b}}{\partial C_L^0} = \frac{K}{(1 + K\gamma C_L^0)^2} \quad (3)$$

The heat of mixing after every injection, δh_i, can then be modeled as (cf. Heerklotz and Seelig, 2000a for details):

$$\delta h_i = C_D^0 \phi' \gamma \cdot \Delta C_L^0 \Delta H_D^{w\to b} \cdot V_0 + q_{dil} \quad (4)$$

TABLE 1 Partitioning and membrane permeabilization data for alkylmaltoside–POPC mixtures

	Dodecyl Maltoside	Tridecyl Maltoside	Tetradecyl Maltoside
Uptake experiments at 10°C			
C_D^0 (mM)	0.05	0.01	0.005
C_L^{syr} (mM)	10	15	10
K (mM^{-1})	3.2	14	46
ΔG^0 (kJ/mol)	−28.5	−31.9	−34.7
$\Delta H_D^{w\to b}$ (kJ/mol)	15	8	3
Q_{dil} (kJ/mol)	−0.1	−0.06	−0.07
$-T\Delta S_D^{w\to b}$ (kJ/mol)	−43.5	−39.9	−37.7
Release experiments at 10°C			
C_D^{syr} (mM)	1	0.8	0.8
C_L^{syr} (mM)	10	10	10
K (mM^{-1})	6.3	18	>46
$\Delta G_D^{0,w\to}$ (kJ/mol)	−30.0	−32.5	
$\Delta H_D^{w\to b}$ (kJ/mol)	9	5	<3
Q_{dil} (kJ/mol)	−0.1	−0.06	
$-T\Delta S_D^{w\to b}$ (kJ/mol)	−39.0	−37.5	
Uptake versus release experiment*			
ΔG_{stress}^0 (kJ/mol)	1.5	0.6	
ΔH_{stress} (kJ/mol)	6	3	
$-T\Delta S_{stress}$ (kJ/mol)	−4.5	−2.4	
Solubilization experiment at 25°C			
C_D^{syr} (mM)	50	50	60
C_L^0 (mM)	10	10	10
$\langle R_b \rangle^{sin}$ (±0.04)	0.17	0.20	0.22
$\langle R_b \rangle^{sat}$ (±0.02)	0.73–0.88	0.81–0.93	0.88–1.0

All fits of uptake and release data (cf. Fig. 2) were performed assuming half of the lipid to be accessible to the alkyl maltosides ($\gamma = 0.5$). The mole ratio surfactant per lipid in the membrane at the local minimum of the observed heat, R_b^{min}, can be assigned to the permeability threshold (see text). The onset of solubilization, i.e., the transition from vesicles to vesicle/micelle coexistence, occurs over a small concentration range as specified in terms of the mole ratio, R_b^{sat}.

*The energetics of stress can be approximately assigned to $\Delta A_{app}/A_0 \approx 20\%$ as argued in the Discussion.

where ΔC_L describes the change in the lipid concentration in the cell of volume V_0 due to an injection, and conservation of mass implies that the mole number of lipid leaving the syringe (injection volume ΔV) equals that arriving in the cell:

$$\Delta n_L = C_L^{syr} \cdot \Delta V = \Delta C_L^0 \cdot V_0 \quad (5)$$

Here, we use an equivalent fit function for the heat normalized per mole of lipid injected, Q, (=NDH in MicroCal terminology) versus $C_L{}^0$ (included in ϕ'):

$$Q \equiv \frac{\delta h_i}{\Delta n_L} = C_D^0 \phi' \gamma \cdot \Delta H_D^{w\to b} + Q_{dil} \quad (6)$$

The molar heat of dilution, Q_{dil}, is assumed to be constant. The fit function Eq. 6 with Eq. 3 has the advantage that it allows varying the injection volume, ΔV, in the course of the titration. We have, typically, used a sequence of one 1-μl injection, three injections of 3 μl, and up to 29 injections of 10 μl each. The heat of the first injection, which is subject to additional errors, was excluded from the fit. The smaller second to fourth injections serve to enhance the resolution in the initial part of the titration, which is particularly useful for rather high partition coefficients.

Release experiment

This protocol serves to quantify the release of bound surfactant upon dilution and to check vesicles for surfactant permeability (Heerklotz et al., 1999). The injection syringe of the calorimeter is loaded with up to 300 μl of a lipid vesicle suspension (10 mM) equilibrated with surfactant (e.g., 0.8 mM) by adding the surfactant solution to the dry lipid followed by vesicle preparation. Then, almost all detergent is bound ($\phi^{syr} \approx 1$ according to Eq. 2, half in the outer and half in the inner monolayer. Hence, the correction factor γ, which takes into account potentially entrapped molecules in the inner monolayer, also applies to the detergent to a good approximation. The cell is filled with buffer so that the first, e.g., 5-μl injection causes a strong dilution of the titrant from $C_L^{syr} = 10$ mM to $C_L^0 \approx 0.035$ mM. As a consequence, ϕ drops from $\phi^{syr} \approx 1$ to $\phi \approx 0$, i.e., all detergent tends to leave the vesicles and the fraction γ will actually do so. The heat of the titration can be modeled by differentiating the bound mole number of detergent with respect to both lipid and detergent because both are varied in the experiment (cf. Heerklotz and Seelig, 2000b for details):

$$\delta h_i = \gamma C_D^0 [\phi' \gamma \cdot \Delta C_L^0 + (\phi - \phi^{syr}) \gamma \cdot \Delta C_D^0] \Delta H_D^{w\to b} \cdot V_0 + q_{dil} \quad (7)$$

It should be noted that Eq. 7 degenerates, except for the factor γ applied to C_D^0, into Eq. 4 if the syringe contains no detergent (uptake experiment, $\Delta C_D^0 = 0$). For the experiments shown here, we use the normalized form of Eq. 7 (obtained analogously to Eq. 6):

$$Q = \gamma C_D^0 [\phi' + (\phi - \phi^{syr}) R^{syr}] \gamma \cdot \Delta H_D^{w\to b} + Q_{dil} \quad (8)$$

where R^{syr} stands for the detergent-to-lipid mole ratio in the syringe, $R^{syr} = C_D^{syr}/C_L^{syr} = \delta C_D^0/\delta C_L^0$.

Solubilization experiment

The aim of this protocol is to measure the enthalpy of transfer of a solute from micelles into lipid membranes and to detect composition-driven phase transitions, i.e., the onset and completion of the vesicle-to-micelle transition (Heerklotz et al., 1995). The cell is filled with a 10 mM lipid vesicle

suspension and these vesicles are titrated with micelles of the solute, 50 or 60 mM (cf. Table 1). The lipid concentration is chosen sufficiently high to ensure a practically complete incorporation of the solute into the membrane so that monomers can be neglected. In our case, $\phi > 94\%$, 98.5%, and 99.5% of the detergent is membrane-bound for C_{12}-, C_{13}-, and C_{14}-maltoside, respectively (cf. Eq. 2). The onset of solubilization is indicated as a sudden drop of the heat of titration, usually from endothermic to exothermic values. The 30-min waiting time after each injection was chosen to ensure that a rather steady state (not necessarily equilibrium) is reached. To enhance the resolution of the transfer enthalpy function at low solute concentration, the injection volumes were varied gradually from 2.9 to 23.5 μl. The measured heats are plotted after normalization with respect to the injected mole number, Δn_L.

NMR measurement of the accessible lipid fraction

A Bruker DRX (9.4 Tesla) wide-bore system with 10 mm broadband observe was used to monitor the ^{31}P signal of vesicle suspensions as used in the ITC experiments. Praseodymium nitrate was added from an isoosmotic stock solution to a final concentration of 5 mM to shift the signal of the lipids on the outer monolayer by ~20 Hz downfield, but leave that of the inner monolayer unchanged (De Kruijff et al., 1976; Frohlich et al., 2001). The FID was acquired after a 30° pulse. Waiting times of 3 s (T1 ≈ 0.7 s) were used to ensure complete relaxation. The field was deuterium-locked (2% D_2O added to sample) and no proton decoupling was performed to avoid an effect of the nuclear Overhauser enhancement on the outside-to-inside intensity ratio.

RESULTS

Uptake and release

Fig. 1 shows the results of uptake and release experiments performed with different alkyl maltosides at 10°C. The uptake of the detergents into the membrane is studied by a titration of vesicles into a detergent solution. It yields endothermic heats of injection (*triangles* in Fig. 1) that decrease gradually when the remaining amount of free detergent becomes less and less. The data sets allow fitting the partition coefficient, K, the molar heat of detergent (D) transfer from water (w) into the bilayer (b), $\Delta H_D^{w\rightarrow b}$, and the small heat of dilution, Q_{dil}, according to Eq. 5 (cf. *solid lines*). The fits were performed assuming that only the outer monolayer, i.e., about half of the total lipid, was accessible to the detergents ($\gamma = 0.5$) and the results are listed in Table 1. If all lipid was accessible to the detergent ($\gamma = 1$), K would be half the value in Table 1.

Release experiments are based on injections of vesicles, preloaded homogeneously with detergent, into buffer. The fit function Eq. 8 with Eqs. 2 and 3 includes the same adjustable parameters as the one for the uptake, so it is possible to predict traces for the release experiment based on the parameters determined upon uptake. These model

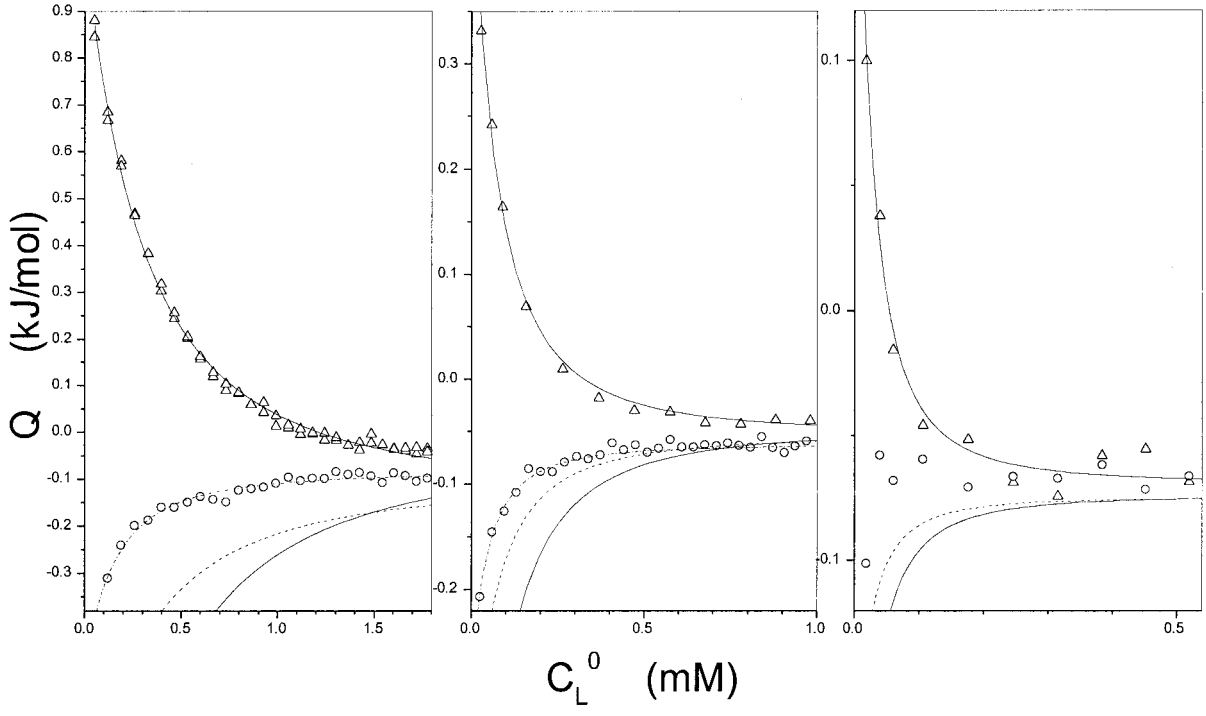

FIGURE 1 Results of ITC uptake (△) and release (○) experiments with POPC vesicles and dodecyl (*left panel*), tridecyl (*middle panel*), and teradecyl maltoside (*right panel*) at 10°C. The measured heats per mole of lipid injected, Q, are plotted versus the lipid concentration, C_L^0, in the cell. The solid lines represent fits of the uptake data according to Eq. 3 using $\gamma = 1$ or $\gamma = 0.5$ (the latter are listed in Table 1). Then, the desired results of the release protocol were simulated according to Eq. 5 and plotted as solid (assuming $\gamma = 1$) and dashed ($\gamma = 0.5$) lines. Free fits to the release data (*dash-dot lines*) yielded the parameters listed in Table 1.

predictions are plotted as solid (assuming $\gamma = 1$) and dashed ($\gamma = 0.5$) lines in Fig. 1. Experiments with permeable detergents have, indeed, revealed a very good agreement of the release data with such a model prediction (Heerklotz et al., 1999; Heerklotz and Seelig, 2000b). Comparing the experimental results for the alkyl maltosides with the model curves, it must be stated that the data are, as expected, closer to the prediction for impermeable membranes. However, there is still a significant deviation. The dash-dot lines correspond to independent fits of the release data (assuming $\gamma = 0.5$) and the corresponding parameters are listed in Table 1. Generally, it turns out that K measured upon uptake is smaller and $\Delta H_D^{w\to b}$ is more endothermic than measured upon release. The release experiment with C_{14}-maltoside gives rise to very small heat values that do not allow a separate fit with reasonable precision. However, qualitative comparison with the dashed curve suggests the same tendencies. The results are given in Table 1, including the free energies of transfer:

$$\Delta G_D^{0,w\to b} = -RT \ln(KC_W) \qquad (9)$$

with

$$C_W = 55.5 \text{ M}.$$

Solubilization protocol

Fig. 2 shows the calorimetric traces and consequent heats of micelle-to-bilayer transfer, $\Delta H_D^{m\to b}$, of an ITC solubilization experiment titrating 10 mM POPC vesicles with a micellar dispersion of 50 mM C_{13}-maltoside. The abscissa is the mean detergent-to-lipid ratio in the membrane, $\langle R_b \rangle$. Fig. 2 resembles the typical behavior of this protocol with an initial range of endothermic heat followed by a sudden jump to exothermic values at the onset of membrane solubilization to micelles (Heerklotz et al., 1995; Heerklotz and Seelig, 2000b). The integrated heat values in the lamellar range (Fig. 2, $\langle R_b \rangle < 0.8$) exhibit a local minimum at $\langle R_b \rangle^{min} \approx 0.2$. Inspection of the raw calorimeter reading (cf. Fig. 2, *top*) reveals that kinetics of surfactant uptake change right at the minimum. Injections before the minimum lead to a fast uptake compared to the instrumental resolution of ≈15 s. At $\langle R_b \rangle^{min}$ (cf. *arrows* in Fig. 2), a second effect with a lifetime of the order of 10 min appears. Subsequent injections exhibit kinetics with an endothermic-exothermic-endothermic sequence. This order persists at higher concentration, but the overall process speeds up again.

The equivalent experiment was performed with C_{12}- and C_{14}-maltoside, and the observed heat values are shown as solid lines in Fig. 3 (identical in *top* and *bottom* panels). The positions of the local minima and the onset of solubilization are given in Table 1.

Another experiment was performed using lipid vesicles that were produced (i.e., extruded) in alkyl maltoside solutions as used for the release protocol. The results were plotted versus the total (titrated plus pre-loaded) $\langle R_b \rangle$ (cf. *dashed lines* in Fig. 3, *top*) and versus the contribution to R_b arising exclusively from the titrated surfactant (*bottom* panel). Note that the onset of solubilization of both pre-loaded and non-pre-loaded vesicles occurs at the same total $\langle R_b \rangle$. In contrast, the local minimum of the heat of titration occurs at the same amount of surfactant titrated into the cell.

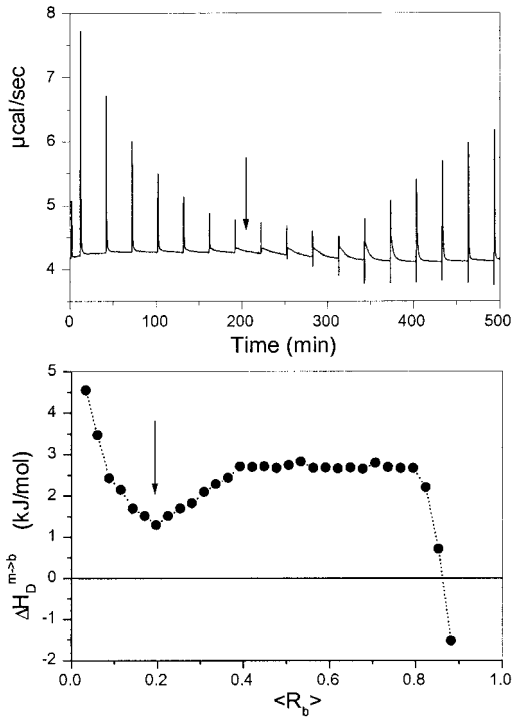

FIGURE 2 Results of an ITC solubilization experiment titrating POPC vesicles (10 mM) with a micellar dispersion of tridecyl maltoside (50 mM). The upper panel shows a detail of the raw data of the compensation heat power versus time. Each injection gives rise to a peak, the area of which is plotted in the lower panel after normalization with the injected mole number. The abscissa of the lower panel is the total surfactant to lipid mole ratio in the sample, $R \approx \langle R_b \rangle$. The composition at the local heat minimum (*arrows*) is denoted $\langle R_b \rangle^{min}$ and that at the sudden drop of the heats is referred to as $\langle R_b \rangle^{sat}$.

NMR experiments

The top trace in Fig. 4 shows the ^{31}P-spectrum of POPC vesicles prepared as described in Materials and Methods. The line is broadened in large vesicles used here (full-width at half-height 250 Hz at 60°C) compared to water-soluble phosphate (6 Hz). Addition of praseodymium nitrate to a concentration of 5 mM does not change the integral intensity (apart from the dilution effect). However, the signal of the lipid that is accessible from the outside is shifted downfield by ≈20 ppm. The signal of lipid localized in the inner monolayer of the vesicles is not shifted. Note that oligola-

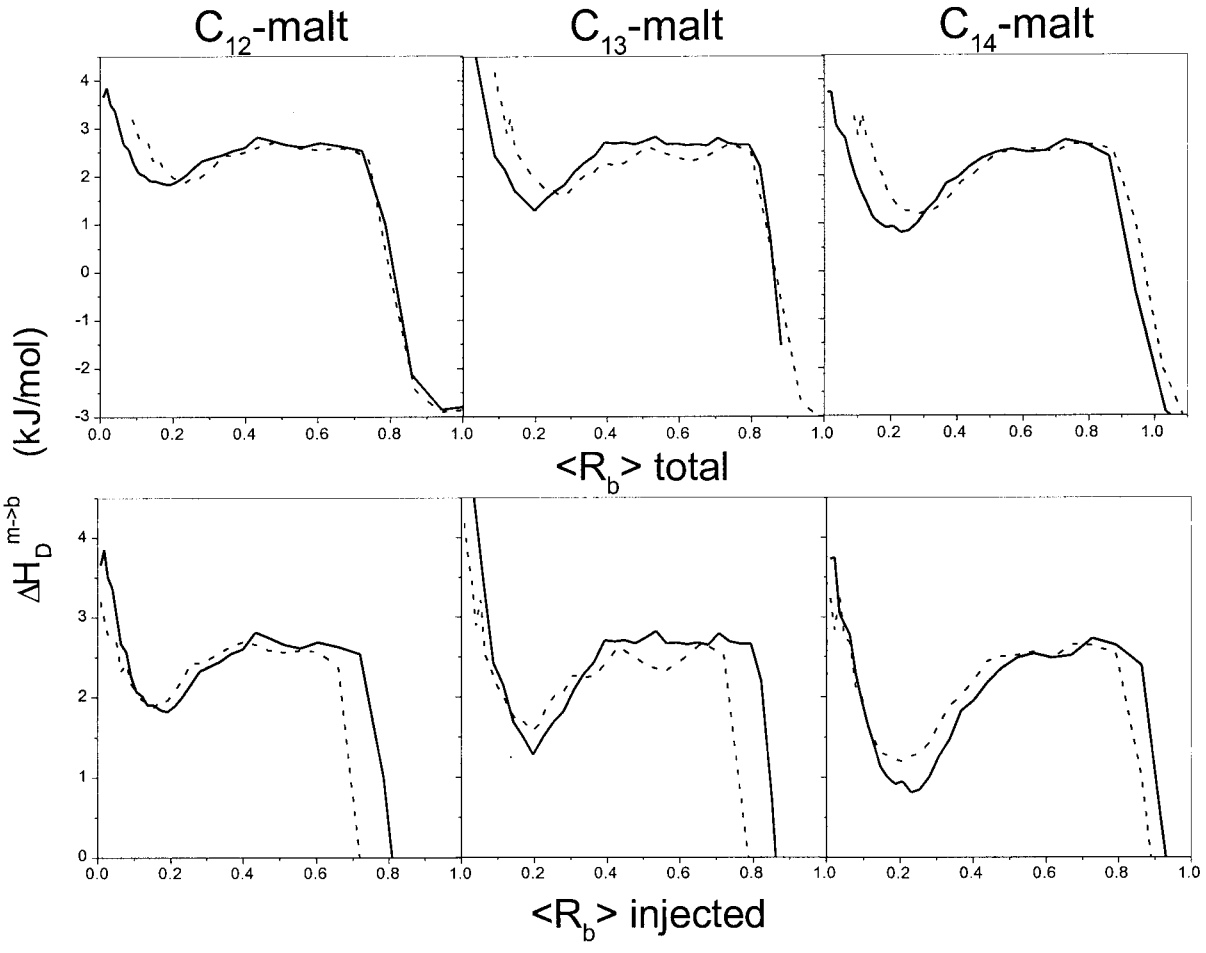

FIGURE 3 Overview of results of ITC solubilization experiments with dodecyl (*left column*), tridecyl (*middle column*), and tetradecyl maltoside (*right column*) as introduced in Fig. 2. Micellar dispersions of alkyl maltosides were titrated into suspensions of POPC vesicles (solid lines) or into POPC vesicles pre-loaded homogeneously with the respective alkyl maltoside $\langle R_b \rangle = 0.1$ for dodecyl and $\langle R_b \rangle = 0.08$ for tridecyl and tetradecyl maltoside) (dashed lines). The top row shows the normalized heat of titration versus the mean (pre-loaded + injected) surfactant content in the sample. The bottom row shows details of the same data re-plotted versus the injected surfactant (ignoring the pre-load). Note that the local minima merge if plotted versus the asymmetrically incorporated surfactant (*bottom row*), whereas the drop from positive (endothermic) to negative values indicating the onset of solubilization is represented by the total R_b (*top row*).

mellar vesicles would expose only one outer monolayer to Pr^{3+}, whereas the signal from all other lipid would remain unshifted.

The integrals under the two well-separated peaks can be directly related to the number of accessible versus inaccessible lipid molecules, yielding an accessible fraction of $\gamma = 0.48 \pm 0.02$ in the present example. The same result is obtained at 25°C, but the substantially broader lines (700 Hz in the absence of Pr^{3+}) lead to some overlap of the outside and inside signal, which requires a deconvolution to determine γ. Repeated vesicle preparations, including those in the presence of 0.8 mM dodecyl maltoside, lead to consistent results. Hence, we may state that deviations from unilamellarity play no substantial role in this study, and $\gamma = 50 \pm 5\%$ of the lipid is exposed to the bulk buffer.

DISCUSSION

Apparent versus real area changes

The techniques introduced here relate the asymmetric incorporation of molecules into vesicles to changes in thermodynamic properties. The perturbation of the system will be quantified in terms of the apparent relative area change per lipid, $\Delta A_{app}/A_0$:

$$\frac{\Delta A_{app}}{A_0} = \frac{\Delta R_b A_D}{A_0} = \frac{\Delta R_b A_D}{A_L + R_b A_D} \tag{10}$$

where the change in the detergent-per-lipid mole ratio, ΔR_b, is weighted by the intrinsic lateral area of the detergent, A_D, and normalized with respect to the relaxed area, A_0. The latter will be given per lipid molecule so that it includes the

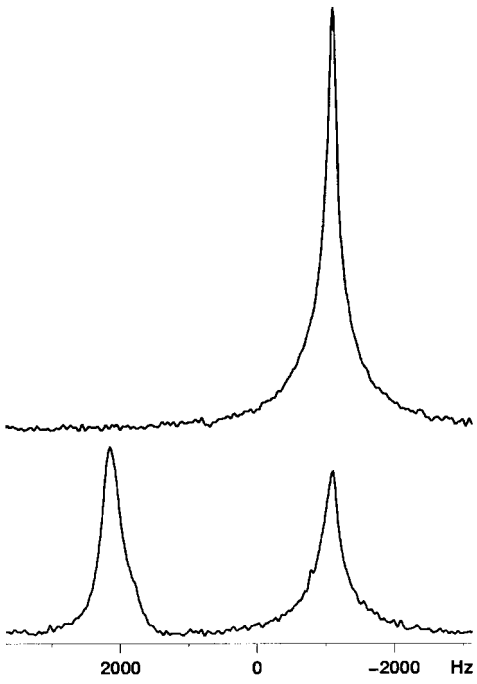

FIGURE 4 ^{31}P-NMR spectra of POPC vesicles prepared as described before (*top trace*) and after (*bottom trace*) addition of 5 mM praseodymium nitrate. The bottom spectrum is split into a line representing the inner monolayer (not shifted) and one representing the outer monolayer (shifted). The areas below both lines agree with each other, implying $\gamma = 0.5$. The same was found in the presence of dodecyl maltoside.

intrinsic lateral area of the lipid, A_L, and the fractional area of the detergent per lipid prior to the perturbation, $R_b A_D$. The areas are assumed as $A_L \approx 65$ Å^2, (Lantzsch et al., 1994) and $A_D \approx 54$ Å^2 measured for dodecyl maltoside on the film balance (X. Li-Blatter, personal communication).

It should be emphasized that $\Delta A_{app}/A_0$ is, in its essence, a measure of the concentration weighted with respect to the intrinsic area. The system will react on asymmetric uptake to the outer monolayer by 1) realizing an area change by increasing bilayer curvature (shape changes, budding) or stretching the inner monolayer; and 2) suppressing monolayer area changes by a strain compressing the area per molecule. Larger vesicles undergo shape changes more easily, whereas smaller ones establish stronger strains. Small asymmetries are essentially covered by smoothing undulations, whereas asymmetries of $>\sim 8$ area-percent induce marked lateral stretching/compression (high-tension regime) (Farge et al., 1990; Evans and Rawicz, 1990; Farge, 1994; Evans and Needham, 1987). Real area changes are quantified in terms of $\Delta A/A_0$. The strain of monolayer compression can also be modeled in terms of a $\Delta A/A_0$, where $-\Delta A$ is just the intrinsic area of the incorporated solute. These effects cannot be monitored by calorimetry. However, $\Delta A_{app}/A_0$ constitutes an interface to relate calorimetric data to information from structural methods and theory. A detailed discussion of the relationship between energetics and structure must be beyond the scope of this paper. A first, crude approximation will be given below.

Comparison of uptake and release data reveals energetics of asymmetry stress

A comprehensive picture of the partitioning behavior is obtained by a parallel application of the classic partitioning protocol (uptake) and the "release" protocol. A very good agreement between the results of both protocols has been reported for surfactants that undergo a fast flip-flop between the outer and inner monolayer relative to the ITC time scale of some minutes ($\gamma = 1$, Heerklotz et al., 1999; Heerklotz and Seelig, 2000b). The large discrepancy between the data and the solid curve in Fig. 1 rules out such fast membrane permeation for the investigated alkyl maltosides. This finding is in accord with the results of Kragh-Hansen et al. (1998). Hence, alkyl maltosides are exclusively taken up into or released from the outer monolayer, respectively.

The remaining discrepancy between the release data and the curve simulated for $\gamma = 0.5$ and the parameters measured upon uptake implies that either 1) K and/or $\Delta H_D^{m\to b}$ differ between uptake and release or, 2) $\gamma \ll 0.5$. To exclude artefacts from multilamellar vesicles ($\gamma \ll 0.5$), which cannot be a priori ruled out in particular for the samples extruded in the presence of surfactant, we have measured the accessible lipid fraction by NMR, yielding $\gamma = 0.5 \pm 0.05$.

Table 1 collects the result of individual fits of Eqs. 6 or 8, respectively, to all uptake and release data assuming $\gamma = 0.5$. In all three cases, the release protocol yields larger partition coefficients and less endothermic transfer enthalpies than the uptake protocol. Such a discrepancy should not occur in the case of equilibrium partitioning. However, asymmetric uptake creates asymmetry stress, the enthalpy of which adds to the enthalpy of (equilibrium) transfer, so that we may write for the effective enthalpy of uptake, $\Delta H_D^{w\to b}$:

$$\Delta H_D^{w\to b}(uptake) = \Delta H_D^{w\to b}(equilibrium) + \Delta H_{stress}(uptake) \quad (11)$$

The effective enthalpy upon release is $\Delta H_D^{b\to w}$ (release):

$$\Delta H_D^{b\to w}(release) = -\Delta H_D^{w\to b}(equilibrium) + \Delta H_{stress}(uptake) \quad (12)$$

Note that the equilibrium transfer is reversed (sign changes with direction) but again, stress is created when detergent is extracted asymmetrically out of an originally relaxed membrane. The universal fit equation (8) generally uses $\Delta H_D^{w\to b}$ for both uptake and release, i.e., Eq. 12 is reversed:

$$\Delta H_D^{w\to b}(release) = \Delta H_D^{w\to b}(equilibrium) - \Delta H_{stress}(uptake) \quad (13)$$

Equations 11 and 13 imply that the difference between the enthalpies obtained by the different protocols is a measure for the sum of the two stress enthalpies:

$$\Delta H_{\mathrm{stress}}(uptake) + \Delta H_{\mathrm{stress}}(release) = \Delta H_{\mathrm{D}}^{\mathrm{w}\to\mathrm{b}}(uptake) - \Delta H_{\mathrm{D}}^{\mathrm{w}\to\mathrm{b}}(release) \quad (14)$$

Analogously, one obtains for the free energy:

$$\Delta G^0_{\mathrm{stress}}(uptake) + \Delta G^0_{\mathrm{stress}}(release) = RT\ln\left[\frac{K(\mathrm{uptake})}{K(\mathrm{release})}\right] \quad (15)$$

To which asymmetry, i.e., to which membrane composition do these statements refer? The membrane composition varies, naturally, in the course of the titration which will, in turn, vary the stress. Then, K and $\Delta H_{\mathrm{D}}^{\mathrm{w}\to\mathrm{b}}$ cannot be strictly constant (as approximated in the evaluation procedure). Model calculations imply that the fit parameters represent in particular the conditions present upon the first injections, which give rise to the largest heat. In our case, that means that the data approximately reflect the situations with the largest asymmetries. We can, thus, tentatively assign the uptake data to membranes with a detergent-per-lipid ratio $R_{\mathrm{b}}^{\mathrm{out}} \approx 0.25 \pm 0.05$ in the outer monolayer, and $R_{\mathrm{b}}^{\mathrm{in}} \approx 0$ in the inner ($\Delta A_{\mathrm{app}}/A_0 \approx 20\%$); and the release data to $R_{\mathrm{b}}^{\mathrm{out}} \approx 0.01$ and $R_{\mathrm{b}}^{\mathrm{in}} \approx 0.08$ ($\Delta A_{\mathrm{app}}/A_0 \approx -5\%$). Because $\Delta H_{\mathrm{stress}}$(release) is supposed to be much smaller than $\Delta H_{\mathrm{stress}}$(uptake) (cf. the next section), we may approximate $\Delta H_{\mathrm{stress}} \approx \Delta H_{\mathrm{stress}}$(uptake) + $\Delta H_{\mathrm{stress}}$(release) and assign this value approximately to $\Delta A_{\mathrm{app}}/A_0$ slightly above 20% (cf. Table 1). The same applies to $\Delta G^0_{\mathrm{stress}}$.

Free energies of membrane stretching upon uptake versus release experiments, theoretical estimate

The elastic free energy contributions of membrane compression/expansion per unit area are described by the relation (Helfrich, 1973):

$$\Delta G^0_{\mathrm{s}} = \frac{1}{2}\,k_{\mathrm{s}}\left(\frac{\Delta A}{A_0}\right)^2 \quad (16)$$

For comparison with ITC data, Eq. 16 must be re-normalized from energy per unit area to energy per mole of detergent added. This is achieved by multiplication with the factor $A_{\mathrm{L}}N_{\mathrm{A}}/\Delta R_{\mathrm{b}}$:

$$\Delta G^0_{\mathrm{s}} = \frac{1}{2}\,k_{\mathrm{s}}\left(\frac{\Delta A}{A_0}\right)^2 \cdot \frac{A_{\mathrm{L}}N_{\mathrm{A}}}{\Delta R_{\mathrm{b}}} \quad (17)$$

where N_{A} is Avogadro's constant. The apparent bilayer stretching modulus in the high-tension regime, which includes contributions from both real area expansion and suppression of undulations, amounts to $k_{\mathrm{s}} \approx 208$ dyn/cm for POPC (Rawicz et al., 2000). Although the monolayer modulus may differ from half the bilayer value, we assume $k_{\mathrm{s}} \approx 100$ dyn/cm $= 0.1$ J/m^2 as a rough estimate for a POPC monolayer in the high-tension regime, which should, at least, apply to the uptake experiments. For the release experiments, which may lead to low-tension systems (Farge, 1994), the use of this value will yield an upper limit of the elastic energy. The modulus for a small compression of a bilayer (e.g., 221 dyn/cm for SOPC, Koenig et al., 1997) is similar to that for expansion.

Let us, for a first approximation, treat the bilayer as a flat surface (thus ignoring shape changes) so that both monolayers are constrained to share the same area. Then, the apparent area change must be accommodated by compression/expansion of the two monolayers, $|\Delta A_{\mathrm{app}}| = |\Delta A^{\mathrm{out}}| + |\Delta A^{\mathrm{in}}|$. The square in Eq. 16 and the similarity of compression and expansion moduli imply that it is energetically cheaper to share the stress between both monolayers than to accommodate all ΔA_{app} exclusively in the monolayer that changes its detergent content.

For the outer monolayer, we assume a compression by $\Delta A^{\mathrm{out}} = -\Delta A_{\mathrm{app}}/2$ upon uptake of $\Delta R_{\mathrm{b}}^{\mathrm{out}}$ detergent molecules per lipid. The corresponding elastic energy is obtained on the basis of Eqs. 17 and 10 as:

$$\Delta G_{\mathrm{s}}^{0,\mathrm{out}} = \frac{1}{2}\,k_{\mathrm{s}}\left(\frac{\Delta R_{\mathrm{b}}^{\mathrm{out}}A_{\mathrm{D}}}{2(A_{\mathrm{L}} + R_{\mathrm{b}}^{\mathrm{out}}A_{\mathrm{D}})}\right)^2 \cdot \frac{A_{\mathrm{L}}N_{\mathrm{A}}}{\Delta R_{\mathrm{b}}^{\mathrm{out}}} \quad (18)$$

The other half of the apparent area asymmetry is balanced by an increase of the total bilayer area, which requires stretching of the inner monolayer: $\Delta A^{\mathrm{in}} = \Delta A_{\mathrm{app}}/2$. Altogether, we obtain:

$$\Delta G^0_{\mathrm{s}} = \frac{1}{2}\,k_{\mathrm{s}}\left[\left(\frac{0.5\Delta R_{\mathrm{b}}^{\mathrm{out}}A_{\mathrm{D}}}{A_{\mathrm{L}} + R_{\mathrm{b}}^{\mathrm{in}}A_{\mathrm{D}}}\right)^2 + \left(\frac{-0.5\Delta R_{\mathrm{b}}^{\mathrm{out}}A_{\mathrm{D}}}{A_{\mathrm{L}} + R_{\mathrm{b}}^{\mathrm{out}}A_{\mathrm{D}}}\right)^2\right] \cdot \frac{A_{\mathrm{L}}N_{\mathrm{A}}}{\Delta R_{\mathrm{b}}^{\mathrm{out}}} \quad (19)$$

Equation 19 suggests an elastic energy of stretching, $\Delta G^0_{\mathrm{s}} \approx 1.4$ kJ/mol for the uptake of $R_{\mathrm{b}}^{\mathrm{out}} \approx \Delta R_{\mathrm{b}}^{\mathrm{out}} \approx 0.25$ into an originally pure lipid bilayer ($R_{\mathrm{b}}^{\mathrm{in}} = 0$), a case which is approximately represented by the uptake experiments in this study. Analogously, one obtains 0.4 kJ/mol for the release ($R_{\mathrm{b}}^{\mathrm{in}} \approx 0.08$, $R_{\mathrm{b}}^{\mathrm{out}} \approx 0.01$, $\Delta R_{\mathrm{b}}^{\mathrm{out}} \approx -0.07$) if the same apparent k_{s} applies to this small perturbation. If effects on undulations, etc. give rise to a low-tension regime also upon asymmetric stretching, ΔG^0_{s} upon release will be even smaller.

The sum of the theoretical estimates, ΔG^0_{s}(uptake) + ΔG^0_{s}(release) ≈ 1.8 kJ/mol is indeed somewhat larger than the experimental values of $\sim\Delta G^0_{\mathrm{stress}} \approx 1.5$ and 0.6 kJ/mol for the different compounds (cf. Table 1), but the significance of the difference is questionable.

Entropic versus enthalpic effects

Little is known about the ethalpic versus entropic contributions to the elastic free energy described by the Helfrich model. We stated above that the asymmetry stress (high-tension regime) is driven by some +3 to +6 kJ/mol of enthalpy and accompanied by an entropic contribution of some −2 to −4 kJ/mol. The interpretation of this finding is not straightforward because asymmetric stress goes along with unknown contributions from local expansion and compression.

Symmetric membrane stretching driven by osmotic inflation of vesicles is endothermic (i.e., opposed by enthalpy) and compression is exothermic (i.e., opposed by entropy) as indicated by direct calorimetric measurements (Nebel et al., 1997). The asymmetric stress (outside compression versus inside stretching, or vice versa) studied here is observed to be opposed by enthalpy.

What are the molecular effects governing this behavior? The positive enthalpy might result from the fact that stretching perturbs the packing of the chains. This effect is endothermic but essentially compensated by entropy gains (Heerklotz and Epand, 2001) and could account for the principle behavior observed here ($\Delta H_D^{w\to b} > 0$, $-T\Delta S_D^{w\to b} < 0$).

A variety of effects may reduce the entropy gain, thus leading to the dominance of enthalpy. 1) Expansion will increase the water-accessible apolar surface area, ASA_{ap}, of the membrane. A net increase of ASA_{ap} by 10 Å^2 per detergent costs entropy of $-T\Delta S_D \approx 1$ kJ/mol, whereas the accompanying enthalpy gain is small at 10°C (Heerklotz and Epand, 2001). 2) Upon membrane compression, the above effect may be overcompensated by the entropy loss upon gradual dehydration of the headgroups (Binder et al., 1999). 3) The restriction or suppression of undulations would also cost entropy.

The asymmetry-controlled permeability threshold

The ITC solubilization protocol (cf. Figs. 2 and 3) yields the molar heat of transfer of a surfactant from micelles to mixed membranes, $\Delta H_D^{m\to b}$, because the experimental conditions ensure almost complete membrane binding of the detergent (cf. Materials and Methods). Such data have been published so far only for detergents that re-distribute quickly across the membrane (cf. Heerklotz and Seelig, 2000b, for a review). Typically, a continuous decrease of $\Delta H_D^{m\to b}$ versus R_b was observed that could be modeled according to regular solution theory, and the membrane perturbation induced by the detergent was the steeper the stronger. For the alkyl maltosides, which do not easily translocate to the inner monolayer, we observe a different pattern exhibiting a local minimum of $\Delta H_D^{m\to b}$ at $\langle R_b\rangle^{min} \approx 0.2$ (cf. Table 1 for details). Based on the models describing composition-dependent enthalpies of detergents in bilayers, it is unlikely that the enthalpy increases again when a certain local detergent concentration is reached. Instead, it must be suspected that addition of detergent (i.e., increase in $\langle R_b\rangle$) leads to a decrease in the local detergent content R_b^{out} which, in turn, increases the enthalpy as usual. This seems a paradox at the first glance but does actually happen at a permeability threshold, when currently added molecules facilitate the translocation of previously added ones from the outer to the inner monolayer.

Let us, for the sake of the argument, imagine 10 injections which increase R_b of a detergent symmetrically in both outer and inner monolayer to 1 and $\Delta H_D^{m\to b}$ linearly (just for simplicity) from 4 to 3 kJ/mol. This case is illustrated by open bars in the background of Fig. 5. What is supposed to happen for a system with the same composition-dependent enthalpy but asymmetric insertion? It exhibits a local detergent content in the outer monolayer, R_b^{out}, which is twice $\langle R_b\rangle$ given in the abscissa. Hence, $\Delta H_D^{m\to b}$ would reach 3 kJ/mol already after five injections and, if the linearity holds, 2 kJ/mol after 10 (*black bars* in Fig. 5). The cumulative heat in the second case (*black bars*) is by 5 kJ/mol smaller, implying that 5 kJ/mol are "stored" in the asymmetric distribution of the surfactant. Now let us assume that a permeability threshold is reached during the 11th injection, which leads all of a sudden to a complete equilibration of the surfactant between the two monolayers. As a consequence, the stored 5 kJ/mol would be released at once and the system would turn to the scenario for symmetric incor-

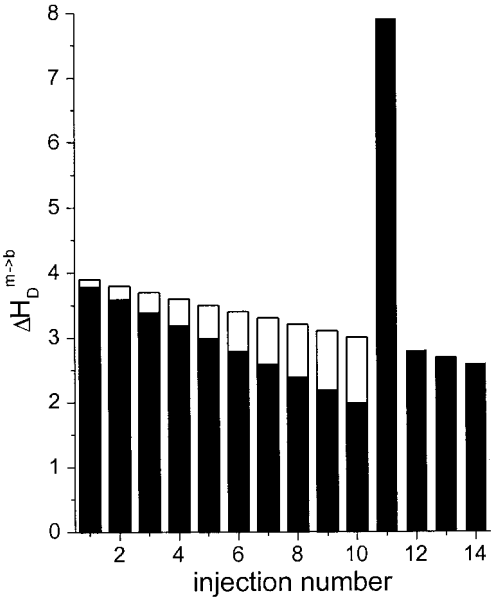

FIGURE 5 Schematic illustration of the consequences of a permeability threshold for the results of an ITC solubilization experiment. The hollow bars in the background refer to the case of a permeable membrane. The black bars describe the subsequent data for the case that the membrane is impermeable to the surfactant for the first 10 injections, but is completely permeabilized during the 11th injection (cf. text for explanation).

poration for subsequent injections, as illustrated. Although sudden complete permeabilization is the extreme case, which is not quite realistic, we may state that a permeability threshold gives rise to a peak and an upward step in the heat of titration.

The experimental data show a local minimum followed by slightly increasing heats over a number of injections. This implies that the local minimum reflects not the total equilibration, but only the onset of a gradual equilibration process. Obviously, only surfactants superseding a certain threshold asymmetry can actually permeate the bilayer, and this threshold is gradually reduced during further injections. Again, we should note that, in terms of kinetics, the onset of permeation in the ITC experiment reflects the situation that permeation gets fast enough to occur within some tens of minutes.

The interpretation of the local minimum of the heat of titration as the threshold for the onset of membrane permeation is fairly compatible with the appearance of a second, slower effect in the raw data (cf. Fig. 2, *top*) mentioned above. Accordingly, the fast process can be assigned to outside incorporation and the slow one to the translocation to the inner monolayer.

Tuning the asymmetry

To study the asymmetry of surfactant incorporation as a function of the mean composition $\langle R_b \rangle$, let us compare systems with the same $\langle R_b \rangle$ but different asymmetries (Fig. 3, *top*) and vice versa (*bottom*). For that purpose, we have repeated the titrations of surfactant micelles into lipid vesicles (Fig. 3, *solid lines*) with vesicles pre-equilibrated with $R_b^{out} = R_b^{in} = 0.08$ of the respective surfactant (*dashed lines*). The top panel shows the resulting heats of titration versus $\langle R_b \rangle$. If the surfactant can equilibrate between both monolayers, it makes no difference whether a surfactant molecule was added before or after vesicle preparation. Then, $\langle R_b \rangle$ suffices to determine the state of the system and the two enthalpy functions should merge. Such a behavior is, in the frame of experimental resolution, observed above $\langle R_b \rangle \approx 0.5$. Notably, this is the typical concentration range where highly curved surfactant-rich structures can form and stabilize membrane leaks by covering the hydrophobic edges (Ueno, 1989; Edwards and Almgren, 1991; Kragh-Hansen et al., 1998; Lasch, 1995). At concentrations $\langle R_b \rangle < 0.4$, however, the dashed traces are up-shifted in $\langle R_b \rangle$ compared to the solid ones. This implies that systems sharing the same $\langle R_b \rangle$ differ in the asymmetry of surfactant incorporation which, in turn, changes their enthalpy.

The bottom panel shows the same enthalpy data, but now plotted versus $\langle R_b \rangle$ of the surfactant added from the injection syringe, ignoring that the samples represented by dashed lines possess an additional 0.08 surfactants per lipid in both monolayers from pre-loading. This abscissa is proportional to $\Delta A_{app}/A_0$ as long as all titrated surfactant remains exclusively in the outer monolayer. It must be emphasized that the local minima of $\Delta H_D^{m\to b}$ merge in this plot, indicating that they are controlled by $\Delta A_{app}/A_0$ rather than by the total $\langle R_b \rangle$. Beyond the minimum, the dashed traces become increasingly down-shifted in $\langle R_b \rangle$. This has to be expected in the case of a surfactant translocation to the inner monolayer, which reduces the asymmetry. We summarize that Fig. 3 provides additional evidence for the idea that the local minimum of $\Delta H_D^{m\to b}$ is asymmetry-controlled and reflects the permeability threshold beyond which a gradual redistribution of surfactant between the outer and inner monolayer occurs.

The local enthalpy minimum $R_b^{min} = 0.17$ observed for dodecyl maltoside appears to coincide with the onset of calcein efflux measured by de la Maza and Parra (1997, 10% dequenching after 40 min at $\langle R_b \rangle = 0.14$, 20% dequenching at $\langle R_b \rangle = 0.28$). A comparison of the behavior of membrane permeation by the surfactant (ITC) and permeabilization to aqueous solutes (calcein) should shed light on the problem whether the translocation of the surfactant to the inner monolayer occurs via a stimulated flip of single molecules across intact membranes or via transient bursts. The latter effect is supposed to play a role for the activity of antimicrobial peptides. However, more detailed studies are required for a conclusive interpretation.

As explained above, we may assign $\langle R_b \rangle^{min} = 0.17$ (i.e., $R_b^{out} = 0.34$) to the permeability threshold for dodecyl maltoside and somewhat larger for the longer-chain analogs (cf. Table 1). The corresponding apparent area asymmetry amounts to $\Delta A_{app}/A_0 \approx 30\%$. It must be emphasized that Farge (1994) reports that "the compression constraint progressively relaxes" after addition of 30% of lysophosphatidylcholine ($\Delta A_{app}/A_0 \approx 30\%$). In their case, permeabilization is discussed to go along with membrane solubilization to coexisting micelles. In our case, permeabilization starts, notably, at the same apparent area asymmetry, although micellization requires substantially higher detergent content, as discussed in the next section. It is an advantage of the new protocol introduced here that both phenomena can be well distinguished. The limiting free energy value for membrane permeabilization estimated according to Eq. 19 with $\Delta R_b^{out} = R_b^{out} \approx 0.4$ and $R_b^{in} = 0$ is ~2 kJ/mol detergent or 0.4 kJ/mol lipid.

Note that symmetric stretching of bilayers upon vesicle inflation leads to mechanical failure of the vesicles already at $\Delta A/A_0 \approx 5$ area-percent (Olbrich et al., 2000). As argued above, symmetric and asymmetric stretching are quite different phenomena.

Vesicle solubilization

The onset of solubilization or lysis of the membrane by the appearance of coexisting mixed micelles is very precisely detected by the ITC solubilization experiment (Figs. 2 and 3) as a sudden drop of the titration heat, often from endo-

thermic to exothermic values (Heerklotz et al., 1995; Heerklotz and Seelig, 2000b). Although the effect is small, it can be considered significant that the limiting surfactant content in bilayers increases with the chain length (cf. Table 1). The value for C_{12}-maltoside is quite consistent with the light-scattering maximum at $\langle R_b \rangle = 0.89$ published by de la Maza and Parra (1997). The chain-length dependence can be explained by the fact that packing problems caused by the chain length mismatch between the lipid and the surfactant destabilize the membrane and, thus, contribute to the driving force for micellization. Similar effects can, for example, be observed comparing the lytic content of $C_{10}EO_7$ ($R_b^{sat} = 0.61$) and $C_{12}EO_7$ (0.72) (Heerklotz et al., 1997; Heerklotz and Seelig, 2000). C_{10}-glucoside does not solubilize POPC membranes at all at room temperatures, whereas C_8-glucoside does (Wenk et al., 1997; Heerklotz and Seelig, 2000).

In contrast to the permeability threshold, the onset of solubilization, $\langle R_b \rangle^{sat}$, by the alkyl maltosides studied here depends only on the mean surfactant concentration. It plays no role whether part of the surfactant has been originally brought into the inner monolayer or all was added from outside (cf. Fig. 3) because the membranes become fully permeable to the surfactant already at sub-lytic concentrations.

Helpful discussions with Prof. J. Seelig are gratefully acknowledged. Many thanks to H. Szadkowska for excellent technical assistance with most ITC experiments, Dr. A. Tölle for technical advice regarding NMR, X. Li-Blatter for measuring the area requirement of dodecyl maltoside on the film balance, and Prof. H. Schmiedel and Dr. T. Wieprecht for important comments.

This work was supported by Swiss National Science Foundation Grant 31.58800.99.

REFERENCES

Bechinger, B. 1999. The structure, dynamics and orientation of antimicrobial peptides in membranes by multidimensional solid-state NMR spectroscopy. *Biochim. Biophys. Acta.* 1462:157–183.

Binder, H., B. Kohlstrunk, and H. H. Heerklotz. 1999. A humidity titration technique to study the thermodynamics of hydration. *Chem. Phys. Lett.* 304:329–335.

Bobrowska-Hagerstrand, M., V. Kralj-Iglic, A. Iglic, K. Bialkowska, B. Isomaa, and H. Hagerstrand. 1999. Torocyte membrane endovesicles induced by octaethyleneglycol dodecylether in human erythrocytes. *Biophys. J.* 77:3356–3362.

Chellani, M. 1999. Isothermal titration calorimetry: biological applications. *Am. Biotechnol. Lab.* 17:14–18.

De Kruijff, B., P. R. Cullis, and G. K. Radda. 1976. Outside-inside distributions and sizes of mixed phosphatidylcholine-cholesterol vesicles. *Biochim. Biophys. Acta.* 436:729–740.

de la Maza, A., and J. L. Parra. 1997. Solubilizing effects caused by the nonionic surfactant dodecylmaltoside in phosphatidylcholine liposomes. *Biophys. J.* 72:1668–1675.

Edwards, K., and M. Almgren. 1991. Solubilization of lecithin vesicles by C12E8. *J. Colloid Interface Sci.* 147:1–21.

Evans, E., and D. Needham. 1987. Physical properties of surfactant bilayer membranes: thermal transitions, elasticity, rigidity, cohesion, and colloidal interactions. *J. Phys. Chem.* 91:4219–4228.

Evans, E., and W. Rawicz. 1990. Entropy-driven tension and bending elasticity in condensed-fluid membranes. *Phys. Rev. Lett.* 64: 2094–2097.

Farge, E. 1994. Scale-dependent elastic response of closed phospholipid bilayers to transmembrane molecular pumping activity—a key for exo-endocytosis physiological process. *Nuovo Cimento Della Societa Italiana Di Fisica D-Condensed Matter Atomic Molecular and Chemical Physics Fluids Plasmas Biophysics.* 16:1457–1470.

Farge, E., M. Bitbol, and P. F. Devaux. 1990. Biomembrane elastic response to intercalation of amphiphiles. *Eur. Biophys. J.* 19:69–72.

Farge, E., D. M. Ojcius, A. Subtil, and A. Dautry-Varsat. 1999. Enhancement of endocytosis due to aminophospholipid transport across the plasma membrane of living cells. *Am. J. Physiol. Cell Physiol.* 45: C725–C733.

Frohlich, M., V. Brecht, and R. Peschka-Suss. 2001. Parameters influencing the determination of liposome lamellarity by ^{31}P-NMR. *Chem. Phys. Lipids.* 109:103–112.

Hagerstrand, H., and B. Isomaa. 1992. Morphological characterization of exovesicles and endovesicles released from human erythrocytes following treatment with amphiphiles. *Biochim. Biophys. Acta.* 1109:117–126.

Heerklotz, H. H., H. Binder, and R. M. Epand. 1999. A "release" protocol for isothermal titration calorimetry. *Biophys. J.* 76:2606–2613.

Heerklotz, H., H. Binder, G. Lantzsch, G. Klose, and A. Blume. 1997. Lipid/detergent interaction thermodynamics as a function of molecular shape. *J. Phys. Chem. B.* 101:639–645.

Heerklotz, H., and R. M. Epand. 2001. The enthalpy of acyl chain packing and the apparent water-accessible apolar surface area of phospholipids. *Biophys. J.* 80:271–279.

Heerklotz, H., G. Lantzsch, H. Binder, G. Klose, and A. Blume. 1995. Application of isothermal titration calorimetry for detecting lipid membrane solubilization. *Chem. Phys. Lett.* 235:517–520.

Heerklotz, H., and J. Seelig. 2000a. Correlation of the membrane/water partition coefficients of detergents with the critical micelle concentration. *Biophys. J.* 78:2435–2440.

Heerklotz, H., and J. Seelig. 2000b. Titration calorimetry of surfactant-membrane partitioning and membrane solubilization. *Biochim. Biophys. Acta.* 1508:69–85.

Helfrich, W. 1973. Elastic properties of lipid bilayers: theory and possible experiments. *Z. Naturforsch.* 28c:693–703.

Huang, H. W. 2000. Action of antimicrobial peptides: two-state model. *Biochemistry.* 39:8347–8352.

Koenig, B. W., H. H. Strey, and K. Gawrisch. 1997. Membrane lateral compressibility determined by NMR and x-ray diffraction: effect of acyl chain polyunsaturation. *Biophys J.* 73:1954–1966.

Kragh-Hansen, U., M. le Maire, and J. V. Moller. 1998. The mechanism of detergent solubilization of liposomes and protein-containing membranes. *Biophys J.* 75:2932–2946.

Lantzsch, G., H. Binder, and H. Heerklotz. 1994. Surface area per molecule in lipid/C12En membranes as seen by fluorescence resonance energy transfer. *J. Fluor.* 4:339–343.

Lasch, J. 1995. Interaction of detergents with lipid vesicles. *Biochim. Biophys. Acta.* 1241:269–292.

Lasch, J., V. R. Berdichevsky, V. P. Torchilin, R. Koelsch, and K. Kretschmer. 1983. A method to measure critical detergent parameters. Preparation of liposomes. *Anal. Biochem.* 133:486–491.

Lindgren, M., M. Hallbrink, A. Prochiantz, and U. Langel. 2000. Cell-penetrating peptides. *Trends Pharmacol. Sci.* 21:99–103.

Longo, M. L., A. J. Waring, L. M. Gordon, and D. A. Hammer. 1998. Area expansion and permeation of phospholipid membrane bilayers by influenza fusion peptides and mellitin. *Langmuir.* 14:2385–2395.

MacDonald, R. C., R. I. MacDonald, B. P. Menco, K. Takeshita, N. K. Subbarao, and L. R. Hu. 1991. Small-volume extrusion apparatus for preparation of large, unilamellar vesicles. *Biochim. Biophys. Acta.* 1061: 297–303.

Mui, B. L., H. G. Dobereiner, T. D. Madden, and P. R. Cullis. 1995. Influence of transbilayer area asymmetry on the morphology of large unilamellar vesicles. *Biophys. J.* 69:930–941.

Nebel, S., P. Ganz, and J. Seelig. 1997. Heat changes in lipid membranes under sudden osmotic stress. *Biochemistry.* 36:2853–2859.

Olbrich, K., W. Rawicz, D. Needham, and E. Evans. 2000. Water permeability and mechanical strength of polyunsaturated lipid bilayers [In Process Citation]. *Biophys. J.* 79:321–327.

Rauch, C., and E. Farge. 2000. Endocytosis switch controlled by transmembrane osmotic pressure and phospholipid number asymmetry. *Biophys. J.* 78:3036–3047.

Rawicz, W., K. C. Olbrich, T. McIntosh, D. Needham, and E. Evans. 2000. Effect of chain length and unsaturation on elasticity of lipid bilayers [In Process Citation]. *Biophys. J.* 79:328–339.

Sackmann, E., H. P. Duwe, and H. Engelhardt. 1986. Membrane bending elasticity and its role for shape fluctuations and shape transformations of cells and vesicles. *Faraday Discuss. Chem. Soc.* 81:281–290.

Schubert, R., K. Beyer, H. Wolburg, and K. H. Schmidt. 1986. Structural changes in membranes of large unilamellar vesicles after binding of sodium cholate. *Biochemistry.* 25:5263–5269.

Schubert, R., H. Jaroni, J. Schoelmerich, and K. H. Schmidt. 1983. Studies on the mechanism of bile salt-induced liposomal membrane damage. *Digestion.* 28:181–190.

Schwarz, S., C. W. Haest, and B. Deuticke. 1999. Extensive electroporation abolishes experimentally induced shape transformations of erythrocytes: a consequence of phospholipid symmetrization? *Biochim. Biophys. Acta.* 1421:361–379.

Shai, Y. 1999. Mechanism of the binding, insertion and destabilization of phospholipid bilayer membranes by alpha-helical antimicrobial and cell non-selective membrane-lytic peptides. *Biochim. Biophys. Acta.* 1462: 55–70.

Sheetz, M. P., and S. J. Singer. 1974. Biological membranes as bilayer couples. A molecular mechanism of drug-erythrocyte interactions. *Proc. Natl. Acad. Sci. USA.* 71:4457–4461.

Uematsu, N., and K. Matsuzaki. 2000. Polar angle as a determinant of amphipathic alpha-helix-lipid interactions: a model peptide study. *Biophys. J.* 79:2075–2083.

Ueno, M. 1989. Partition behavior of a nonionic detergent, octyl glucoside, between membrane and water phases, and its effect on membrane permeability. *Biochemistry.* 28:5631–5634.

Vogt, B., P. Ducarme, S. Schinzel, R. Brasseur, and B. Bechinger. 2000. The topology of lysine-containing amphipathic peptides in bilayers by circular dichroism, solid-state NMR, and molecular modeling. *Biophys. J.* 79:2644–2656.

Wenk, M. R., T. Alt, A. Seelig, and J. Seelig. 1997. Octyl-beta-D-glucopyranoside partitioning into lipid bilayers: thermodynamics of binding and structural changes of the bilayer. *Biophys. J.* 72:1719–1731.

Wieprecht, T., M. Beyermann, and J. Seelig. 1999. Binding of antibacterial magainin peptides to electrically neutral membranes: thermodynamics and structure. *Biochemistry.* 38:10377–10387.